南京航空航天大学

论文集

（二〇一〇年） 第32册

民航学院

（第2分册）

南京航空航天大学科技部编

二〇一一年五月

民航学院

072～074

A Metric for Air Traffic Complexity

Zhang Chen*, Hu Minghua, Zhang Jing

[1]Civil Aviation College, Nanjing University of Aeronautics and Astronautics, Nanjing 210016, China

Abstract

As ATM system has become more congested with proliferated demands, and preferred trajectories own higher priorities than before, it's necessary to develop integrated metrics for daily operation. To gain insight of the traffic orderly status, the paper proposes a multi-dimensional complexity metric focusing on the unsymmetrical effects imposed by the inter-relationship emerged among the multi-aircraft pair-wise. The proximity effects on the individual aircraft based on the single-aircraft and multi-aircraft pair-wise are modeled and the difference between them inspires us to present the synchronization structure of the traffic considering the traffic patterns in controllers' minds. Then a new metric for traffic complexity is set up and initially validated under typical static traffic situations. We find it's good for revealing the availability of shady airspace, so two kinds of re-route strategies with corresponding simulation scenarios are discussed. It's easy to excavate the potential airspace capacity with the metric and both the heading and the clearance of the interval period adjusting strategies can be found maintaining acceptable complexity level as well, which implies the application field of the new metric for future dynamic ASM and ATFM.

Keywords air traffic control, complex systems, air traffic pattern; airspace capacity management, re-route strategy

1. Introduction

Airspace means nothing itself without air traffic in some sense and the attributes of the traffic can be used measuring airspace performance. Metrics for traffic complexity become the base of capacity and trajectory management and some of them have been validated. G. B. Chatterji and B. Sridhar defined a metric by neural network method and proved its suitability for high density airspace[1]. D. Delahaye, S. Puechmorel, et al. investigated some metrics based on intrinsic parameters of aircraft, considered the flow structure and captured its disorder degree in the organization of 4D trajectories[2-3]. M. A. Ishutkina and E. Feron introduced a linear programming solver to find the smooth vector field satisfying aircraft performance constraint to analyze the relationship between airspace and its traffic[4]. K. Lee investigated airspace responses towards traffic disturbances through sketching complexity maps[5]. These metrics are macro-level and neglect the heterogeneity of the traffic for TBO concepts. So the paper proposes a metric from a middle-level viewpoint, validates its effectiveness for airspace performance characterization.

2. New Metric for Air Traffic Complexity

2.1 *Descriptive dimensions reduction*

The complexity ofthe air traffic significantly emerges from the patterns combinatorial blast of the relationships among aircraft. Those relationships mainly involve space-time information concerning all the individual aircraft. Metric modeling should well deal with reduction of descriptive dimensions while maintaining enough information for decision making. This section introduces the approach to combine the space and time dimensions into one considering the proximity effects on the individual aircraft based on the single-aircraft and multi-aircraft pair-wise.

Aircraft's ground speed and position are undoubtedly the intrinsic attributes for facilitating direct observation, and are most concise representation of the time and space dimensions of the traffic pattern at any period. Because no conflict could be beard under any circumstances, and the minimum separation criterion should be maintained, degree of urgency for the operational staff to deal with the traffic could be reflected in some sense by the proximity level of an aircraft pair-wise. Towards a single-aircraft pair-wise, the relative distance can be defined as D_{ij}, and the relative speed can be defined as V_{ij}, which are the simplest relationship of two aircraft. D_{ij} reflects instant spatial occupancy extent of two aircraft, and V_{ij} reflects the time duration for the aircraft to be safely separated. Both of them characterize the most details of the proximity status of the aircraft pair-wise. To reduce the descriptive dimensions of air traffic, considering the common danger consciousness, we combine D_{ij} and V_{ij}

* Corresponding author. E-mail address: wskkdxy@126.com

Foundation item: National ATM Scientific Research Program of China (GKG200802006)

factors for each aircraft pair-wise to set up PE_{ij}^{s} representing proximity effects.

D_{*p} is the minimum separation criterion, and no violation can be made. Therefore the D_{ij} of an aircraft pair-wise is critical for traffic situation presentation. We consider the proximity effects caused by D_{ij} can be expressed as an inverse ratio to D_{*p}. However, there exists a threshold which defines a specific relative distance with little effects on both aircrafts in a pair-wise. So those D_{ij} below the median value of all D_{ij} for aircraft i are useless and neglected in the data process. (D_{ij} , V_{ij}) is inner product of D_{ij} and V_{ij}. (D_{ij} , V_{ij})/ | D_{ij} | is the projection of the vector V_{ij} on the vector D_{ij}. The effects of V_{ij} are to emphasize those effects imposed by the D_{ij}. We consider proximity effects caused by V_{ij} as the direct ratio to that of the maximum V_{ij} for all aircraft i. and those V_{ij} below the average value of all V_{ij} are neglected either. Then, PE_{ij}^{s} is the sum-up of those effects by V_{ij} and D_{ij} discussed above. The principle is that the further two aircraft are apart, the smaller effects they will make on each other, and the faster two aircraft approach, the more urgent the CD&R should be taken. PE_{ij}^{s} is to reduce the descriptive dimensions for a single-aircraft pair-wise and synthesizes the time-space traffic factors into a micro-level situation indicator. However, in real daily operation, the decision maker onboard or on the ground focuses mostly on the allocation in interactions among aircraft, and the local traffic has the most significant impacts on various decisions making. So we consider the influences towards the individual aircraft from its surrounding traffic are more important than those influences from the traffic far away. For an aircraft, another aircraft possessing the most proximity effects have the maximum correlation with it, and producing the maximum occupation tendency upon it. So the influences of such correlation decrease along with the reduction of the proximity effects. We define the weight of each PE_{ij}^{s} for aircraft i as follows:

$$\left(\frac{PE^{s}}{\max(PE^{s})}\right)^{c} = \frac{W^{PE}}{M}, \quad j \neq i, \quad 0 < c < 1 \quad (1)$$

In formula (1), c is an adjusting parameter, and M is a predefined constant parameter. Then we define PE_{ij} with W_{ij}^{PE} considering distributed decision making preference and PE_{ij} can be expressed as below:

$$PE_{ij} = PE^{s} \cdot W^{PE} \quad (2)$$

2.2 Asymmetric information caused disorder

As a status indicator of the minimum component of air traffic, PE_{ij}^{s} emphasizes the absolute impacts imposed by a couple of aircraft each other. Therefore, the relationship matrix composed of PE_{ij}^{s} is symmetric, which means the information shared between the aircraft is no difference in each aircraft's decision making process. However, PE_{ij} emphasizes the relative proximity effects towards one aircraft by the other one due to multi-aircraft pair-wise situation and information becomes different for each aircraft of a pair-wise because the focus scope is refined respectively as the traffic descriptive dimensions are further reduced. W_{ij}^{PE} in fact represents the degree of the available information for an aircraft according to its local traffic patterns. Hence the relationship matrix composed of W_{ij}^{PE} is asymmetric, which reflects the distributed structure of the space-time information of the overlapped local traffic situations for various individual aircraft. W_{ij}^{PE} is suitable for hybrid operational environment, which is common as decision makers in the same system have limited cognitive resource and control assets simultaneously.

W^{PE} differentiate the value of the same proximity information for two aircraft in an aircraft pair-wise. The degree of such differentiation can be expressed by the standard deviation of W_{ij}^{PE} and W_{ji}^{PE} and we use it, namely S_{ij}, as the indicator of the skewness of mutual traffic information of an aircraft pair-wise. The larger S_{ij} is, the more difference the same PE_{ij}^{s} is regarded in the local decision making, and the more relationship asymmetry caused by different overlapped traffic situations involving different traffic structures. Therefore, S_{ij} not only sets up a local information distribution map, but also presents the disorder degree of the micro-level air traffic in a sense of information usage. That is to say, if the same information takes similarly important effects in the decision making, the degree of the cooperation among stakeholder will be easier, or else the evolution of the traffic situations will be more difficult to predict and control, and leads to chaos more easily. Such uncertainties will cause the asynchronism and emergent complexity of the air traffic.

2.3 Synthesized complexity metric

To build up a synthesized indicator reflecting the aircraft pair-wise nexus based on information distribution bifurcation, we define G as the median of all the S_{ij} to reflect synchronization status of the air traffic. G is not defined as the maximum of the S_{ij} because we aim at middle-level metric modeling excluding extreme situation and G is not defined as the average of the S_{ij} either because average value may shield salient asymmetry, which is exactly the detail the metric should presents in focus. For the same reason, the synthesized indicator reflecting the aircraft pair-wise nexus entirely on the base of proximity effects is defined as the median of all the PE_{i}^{s}, namely P, while PE_{i}^{s} is the maximum value of PE_{ij}^{s} because the aircraft j involved is most critical in CD&R for operation safety. With the indicators set up above, we define the synthesized complexity metric as $C = G \cdot P$.

3. Initial Validation-Static Traffic Situations

4 typical static traffic situations commonly used in the complexity research are shown as Fig. 1, and the

speed of all aircraft is set 420 knot. The complexity values are 2.7071(2.7071, 1), 1.2929(1.2929, 1), 1.9386(2.25, 0.8616), and 2.1464(2.1464, 1) respectively. Two values in the parenthesis are P and G. Because the situation 3 consists of divergent and convergent aircraft simultaneously, its G is lower than other 3 situations, which are totally symmetric, and its P is greater than situation 2 & 4. Situation 2 only consists of 4 divergent aircraft with lowest proximity effects, so it has the minimum complexity value.

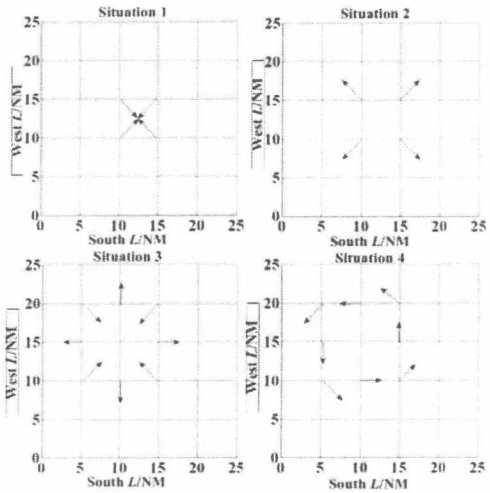

Fig. 1 Static traffic situations 1 - 4

Based on the situation 1, we add an additional aircraft at specific position of different distances far from the focused area. As the new aircraft locates at coordinate (19, 19) with heading 180 deg, the complexity value decreases from 2.707 1 to 1.215 1. As the aircraft withdraws along the diagonal line towards north-east with heading unchanged, the complexity values non-linearly decrease gradually to a specific level 1.075 3. Extra aircraft confirms more available airspace outside the focused airspace used to exist, expanding the current focused area to a larger space with relative smaller density. So the complexity level of situation with additional aircraft is lower than that of situation 1 with 4 A/C counts. And the specific locations with complexity values 1.075 3 outside the focused airspace make little effects on it, which separate the traffic into two parts. The boundary formed by these locations reflects the objective behavior as the reaction of the focused airspace to the outside traffic situations. Radical behavior would expand the scope of the original focused airspace to hold new coming traffic, combine it with existing traffic flow and renew structure of the traffic situation inside it smoothly, which results in the increase of the capacity of available airspace. And passive behavior concerns to traffic conflicts. If variance in traffic causes sharp rise in complexity level, traffic structure in the original focused airspace would place a significant negative coupling with the new traffic to make the situation alienation, and the extension of the original focused airspace to new one will make it more difficult to re-arrange the traffic and re-configure the airspace structure. The difficulty implies conflict reactions of the original focused airspace to the adjusting actions, such as imposing stringent restrictions to the downstream sector to reduce airspace usage flexibility.

StaticSituations preliminarily validates the effectiveness of the new metric in the middle-level decision making. It's quite fit for sketching the structure and organization of the traffic in all situations, which are emphasized in real operation and regarded as elemental attributes of airspace system. Therefore, the new metric is quite meaningful for further exploration towards the characterization of airspace performance.

4. Further Validation—Re-route Cases

We set up a rectangle sectorwith 2 convergent routes. The entries of 2 routes are located at points (0, 70) and (0, 30). The convergent point is located at the point (30, 50) and the exit of 2 routes is at the point (50, 50). Ground speed is set 420 knot for all the aircraft. Input streams of 2 routes are separated with the clearance of the interval period of 15 time frames and 200 aircraft are set to fly over each route. Assumes 100 aircraft of the adjacent sector with the clearance of the interval period of 15 time frames should re-route and find new route from (0, 0) to the right edge of the sector at the 300 time frame.

As the exit point of the re-route path is at (50, 1), the values of aircraft counts and complexity metric are recorded shown in Fig. 2. It's interesting the complexity level descends when the re-route aircraft in the sector simultaneously increase to 4 or 6 because the new traffic flow gradually expands the range of focused airspace filling blank area with no complexity factors and make the average level of the traffic complexity drop a little. Such drop obviously forms a concave in complexity values between time frames 300 and 1 500, which implies the fact that original airspace structure owns attractive effects on the surrounding traffic. If we can fill the groove by adjusting the re-route clearance of the interval period or the re-route heading, more capacity might be excavated for demands of adjacent sectors, and airspace performance could be sketched more accurately in such situations.

2 common strategies setting up the available re-route path are to adjust the clearance of the interval period and the entry/exit position. We firstly set the initial import time of re-route aircraft with heading 0 deg at 300 time frames and the clearance of the interval period as 15 time frames. We gradually change the reroute entry/exit positions until the complexity concave of the original focused airspace is filled up. As re-route entry/exit positions reach (0, 23) & (50, 45), the

complexity curve is stable and almost in line with that of the original airspace structure, shown as Fig. 3 (b). So we consider the points (0, 23)/ (50, 45) as critical entry/exit positions. Those points different from such position own less or greater complexity values than that of the original complexity curve, and 2 of them are shown as Fig. 3 (a) & (c).

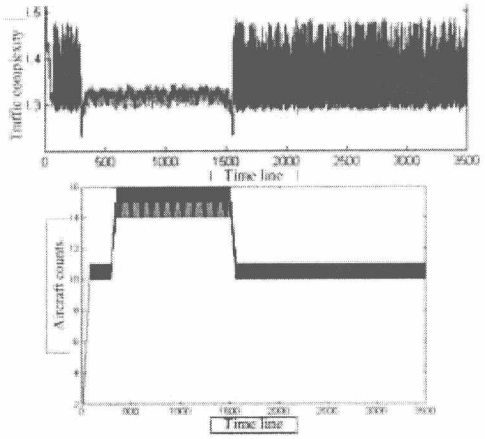

Fig. 2 Aircraft counts . vs. complexity metric

We further discuss the strategy of adjusting the clearance of the interval period. As the clearance of the interval period decreases gradually, the peak values of the complexity metric as to the re-route traffic situation have a monotone increasing trend. Assumes the re-route entry/exit positions are set (0, 0) & (50, 1), as the clearance of the interval period gradually reduces less than 12, the concave obviously fills up the complexity concave, shown as Fig. 4. So the clearance of the interval period also has a critical value. The complexity level of the original blank area soars and exceeds the effects of the traffic in original focused airspace as the re-route clearance of the interval period being much smaller, which results in the rush of the complexity of the overall airspace. Hence the re-route flow may disrupt the original traffic structure and the sharp rise in complexity indicates that the sector would exclude the corresponding re-route flow.

5. Conclusion

Amulti-dimensional metric for air traffic complexity is modeled for synthesizing space-time attributes of aircraft, reducing descriptive dimensions of the traffic, characterizing information distribution based decision making mode. Its application solving re-route problem is discussed and the critical adjusting strategies of the heading and the clearance of the interval period are obtained, which validate the effectiveness of the new metric for the decision making tools development for the future air traffic management concepts.

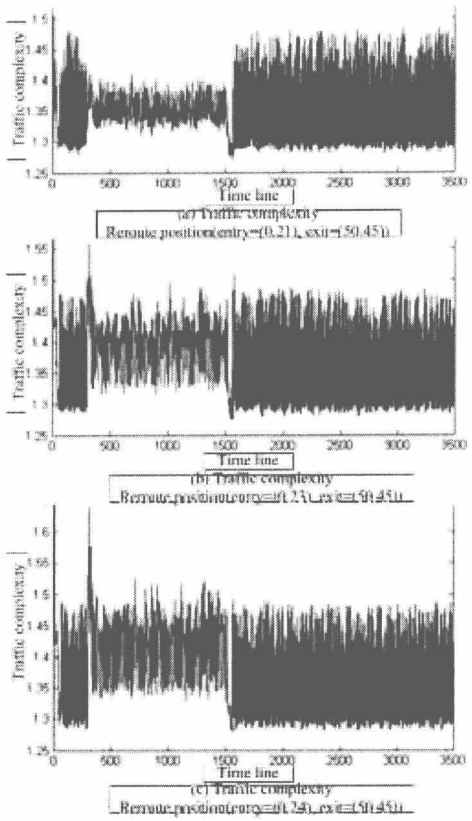

Fig. 3 Traffic complexity (reroute entry/exit positions)

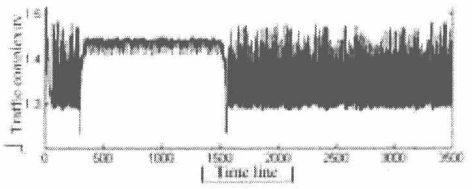

Fig. 4 Traffic complexity (reroute interval period=12)

References

[1] Chatterji G B, Sridhar B. Measures for air traffic controller work-load prediction. Proceedings of the First AIAA Aircraft Technology, Integration, and Operations Forum. AIAA - 2001 - 5242, 2001:1 - 14.

[2] Histon J M, Hansman R J, Aigoin G, Delahaye D, Puechmorel S. Introducing Structural Considerations into Complexity Metrics. Air Traffic Control Quarterly. 2002,10 (2):115 - 130.

[3] Delahaye D, Puechmorel S, Hansman R J, Histon, J M. Air traffic complexity based on non linear dynamical systems. Air Traffic Control Quarterly. 2004,12(4): 367 - 388.

[4] Ishutkina M A, Feron E, Bilimoria K D. Describing air traffic complexity using mathematical programming. AIAA 5th Aviation, Technology, Integration and Operations Conference. AIAA 2005 - 7453, 2005:1 - 9.

[5] Lee K. Describing airspace complexity: airspace response to disturbances. PhD thesis, Georgia Institute of Technology, 2008.

文章编号：0258-2724(2010)02-0261-07 DOI：10.3969/j.issn.0258-2724.2010.02.017

基于动态容量的航班进离场流量鲁棒优化分配

杨尚文， 胡明华
（南京航空航天大学民航学院，江苏 南京 210016）

摘 要：为解决机场和定位点动态容量条件下的航班进离场流量优化分配问题，以总航班延误损失为决策依据，建立了绝对鲁棒优化模型、偏差鲁棒优化模型和相对鲁棒优化模型，并用捕食搜索算法，设计了寻找鲁棒最优解的算法流程. 以国内某机场数据为例进行仿真验证，结果表明，得到的鲁棒最优解能够根据不同偏好有效规避风险，与该终端区一般容量条件下最优解的航班延误损失相比，偏差鲁棒最优策略和相对鲁棒最优策略下的航班延误损失分别减少了8.2%和7.8%.

关键词：空中交通管理；流量分配；鲁棒优化；捕食搜索算法；动态容量
中图分类号：V355.1 **文献标识码**：A

Robust Optimization of Aircraft Arrival and Departure Flow Allocation Based on Dynamic Capacity

YANG Shangwen， *HU Minghua*
(College of Civil Aviation, Nanjing University of Aeronautics and Astronautics, Nanjing 210016, China)

Abstract: To optimize the allocation of aircraft arrival and departure flow under dynamic capacity of airports and fixes, an absolute robust optimization model, a deviation robust optimization model, and a relative robust optimization model were built, where the objective function is to minimize the total cost of delayed flights. Then, a solution process based on predatory search algorithm was developed to solve the robust optimization problems. A case study regarding the operation of one of Chinese airports was performed to verify the models. The simulation results show that the robust optimal solutions produced from these models could effectively avoid risks on the basis of different decision preferences in actual operations; compared with the optimal solution under the capacity of terminal area with common conditions, the strategy of deviation robust optimization could reduce the delay cost by 8.2%, and the strategy of relative robust optimization could reduce the delay cost by 7.8%.

Key words: air traffic management; flow allocation; robust optimization; predatory search algorithm; dynamic capacity

航班进离场流量分配是根据空中交通需求和机场容量，协调分配流量，优化利用容量，从而最小化航班延误的空中交通流量管理策略. 传统的空中交通战略流量管理将进场和离场视为两个相互独立的过程，并将机场容量视为恒定值[1-2]. 实际上进场和离场是相互影响与制约的两个过程，进场容量和离场容量一般表示为图1的机场容量曲线[3]，且随天气条件变化. 当交通需求超过机场容量时，应在容量曲线上或其下方寻求Pareto最优的点，从而最小化航班延误. 文献[4]根据最小化进离场队列中延误的航班量建立流量分配模型. 文献[5]研究了定位点和跑道容量限制下的终端区流量优化分

收稿日期：2009-07-26
基金项目：国家863计划重点项目(2006AA12A105)
作者简介：杨尚文(1984－)，男，博士研究生，研究方向为空中交通流量管理，电话：15062265692，E-mail：swyang_08@yahoo.cn
通讯作者：胡明华（1962－），男，教授，博士，E-mail：minghuahu@263.net

配问题,指出在需求接近或超过容量时,进离场流量分配应同时考虑机场容量和定位点容量的约束.文献[6]通过分析跑道容量和走廊口容量的相互影响分配流量.文献[7]以航班延误时间最短为目标建立了流量分配的动态规划模型.文献[8]基于CDM(collaborative decision making)思想,考虑航空公司利益,通过加入航班优先级研究流量协同优化策略.文献[9-10]考虑了航班类型、重要程度、航空公司利益等因素,结合CDM思想,以航班延误损失最小为目标建立了模型.文献[11]引入满意度准则,通过分析跑道容量和定位点容量的相互影响,以容量利用满意度和机场系统流量最大化为目标,建立了多目标优化模型.

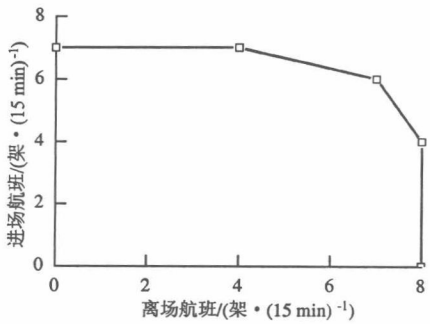

图1 机场容量曲线
Fig. 1 Airport capacity curve

机场和定位点容量虽然与机型比例、空管规则、机场构型、航路结构等因素有关,但动态容量受天气条件等不确定因素的影响显著.对未来较短时间内的流量分配,应根据动态容量评估与预测结果进行.因此,基于动态容量的空中交通战术或预战术流量管理具有更重要的实际意义.

由于天气等随机因素的复杂性和不确定性,难以得出准确的动态容量,但可以预测其分布区间[12].现有的研究成果一般基于静态容量,难以适应空中交通战术或预战术流量管理的要求.文献[11]虽然引入了机场和定位点的容量区间,但各时段的容量区间相同,未反映出容量的动态变化,仍为一种静态容量,各时段的满意度函数也相同,因此,该文献仍然是基于静态容量的流量分配研究.有效的空中交通流量管理建立在对容量准确评估的基础上.动态容量评估是目前空管研究的前沿之一.

本文在已知动态容量预测区间的条件下,以航班延误损失为决策依据,建立了进离场流量分配的鲁棒优化模型,设计了基于捕食搜索算法的求解方法,所求方案为空中交通战术流量管理提供了有效的决策依据.

1 问题描述

流量分配的根本目的是平衡需求与供给,减少航班延误.在已知不同天气状况下的机场容量曲线、未来某时间区间内的空中交通需求、该时间区间内的机场和定位点动态容量区间的条件下,为了优化容量利用,将航班延误损失[10]作为决策依据,寻求具有较强鲁棒性、适应不同决策偏好的流量分配方案.

设待优化的时间区间 T 由 n 个长度为 ΔT 的时段组成,$T=\{t_1,t_2,\cdots,t_n\}$;F_A 为 T 内的进场航班集合,$F_a\in F_A$;F_D 为 T 内的离场航班集合,$F_d\in F_D$;$J_{arr}=\{1,2,\cdots,J\}$ 为进场定位点集合;$K_{dep}=\{1,2,\cdots,K\}$ 为离场定位点集合.对于任意 $t_i\in T$,$j\in J_{arr}$,$k\in K_{dep}$,$F_{Aj}(t_i)$、$F_{Dk}(t_i)$ 分别为时间段 t_i 内进场定位点 j 和离场定位点 k 的容量;$D_{Aj}(t_i)$、$D_{Dk}(t_i)$ 分别为时间段 t_i 内进场定位点 j 和离场定位点 k 的空中交通需求;$x_{Aj}(t_i)$、$x_{Dk}(t_i)$ 分别为时间段 t_i 内进场定位点 j 和离场定位点 k 的流量;$X_A(t_i)$、$X_D(t_i)$ 分别为时间段 t_i 内分配的进场流量和离场流量;$h_A(t_i)$、$h_D(t_i)$ 分别为时间段 t_i 内的进场容量和离场容量;$H(t_i)$ 为时间段 t_i 内的机场容量;$h_{A\min j}(t_i)$、$h_{A\max j}(t_i)$ 分别为时间段 t_i 内进场定位点 j 的最小容量和最大容量;$h_{D\min k}(t_i)$、$h_{D\max k}(t_i)$ 分别为时间段 t_i 内离场定位点 k 的最小容量和最大容量;$h_{\min}(t_i)$、$h_{\max}(t_i)$ 分别为时间段 t_i 内机场的最小容量和最大容量.$C_f(t_i)$ 为航班 f 在时间段 t_i 内进场或离场的延误损失函数[10],定义

$$C_f(t_i)=c_f(t_i-e_f)^{1+\varepsilon},$$

其中:c_f 是航班 f 的延误损失优先级系数,代表单位时间的延误损失,由航班机型、重要程度等因素决定;e_f 为航班 f 的预计进场或离场时间;参数 ε $(0<\varepsilon<1)$ 表示航班延误成本的缓慢超线性增长,能避免过多地延误某一航班;$C_f(t_i)$ 综合了各种航班因素,所确定的延误损失为无量纲量.目标函数为:

$$\min \sum_{F_a\in F_A}\sum_{t_i\in T}C_a(t_i)\delta_a(t_i)+\sum_{F_d\in F_D}\sum_{t_i\in T}C_d(t_i)\delta_d(t_i), \tag{1}$$

式中:

$$\delta_a(t_i)=\begin{cases}1, & \text{航班 } F_a \text{ 在时段 } t_i \text{ 进场},\\ 0, & \text{否则},\end{cases}$$

$$\delta_d(t_i)=\begin{cases}1, & \text{航班 } F_d \text{ 在时段 } t_i \text{ 离场},\\ 0, & \text{否则},\end{cases}$$

约束条件为:

$$X_A(t_i)=\sum_{F_a\in F_A}\delta_a(t_i), \tag{2}$$

$$X_D(t_i)=\sum_{F_d\in F_D}\delta_d(t_i), \tag{3}$$

$$\sum_{j=1}^{J}x_{Aj}(t_i)=X_A(t_i),\quad x_{Aj}(t_i)\leqslant F_{Aj}(t_i), \tag{4}$$

$$\sum_{k=1}^{K}x_{Dk}(t_i)=X_D(t_i),\quad x_{Dj}(t_i)\leqslant F_{Dk}(t_i), \tag{5}$$

$$X_A(t_i)\leqslant h_A(t_i),\quad A_D(t_i)\leqslant h_D(t_i), \tag{6}$$

$$\alpha(t_i)X_A(t_i)+\beta(t_i)X_D(t_i)\leqslant\gamma(t_i), \tag{7}$$

$$\left.\begin{aligned}&h_{A\min j}(t_i)\leqslant F_{Aj}(t_i)\leqslant h_{A\max j}(t_i),\\ &h_{D\min k}(t_i)\leqslant F_{Dk}(t_i)\leqslant h_{D\max k}(t_i),\end{aligned}\right\} \tag{8}$$

$$\left.\begin{aligned}&h_{\min}(t_i)\leqslant H(t_i)\leqslant h_{\max}(t_i),\\ &F_{Aj}(t_i),F_{Dk}(t_i),H(t_i)\in N.\end{aligned}\right\} \tag{9}$$

式(2)和(3)分别表示时间段 t_i 内的进场流量和离场流量约束;式(4)和(5)分别为时间段 t_i 内的定位点容量约束;式(6)和(7)分别为时间段 t_i 内的机场容量约束,$\alpha(t_i)$、$\beta(t_i)$、$\gamma(t_i)$为容量曲线系数;式(8)和(9)为时间段 t_i 内机场和定位点的动态容量区间.

2　鲁棒优化模型

常用的处理不确定优化问题的方法有随机优化、模糊优化、鲁棒优化等. 随机优化要求已知不确定参数的概率分布,模糊优化则要求已知其隶属度函数,无论是概率分布还是隶属度函数在实际中都难以准确掌握,影响了这两种优化方法的应用. 鲁棒优化是解决不确定优化问题的有效方法,已得到广泛应用[13]. 当未来可能发生的情景不唯一,并且各种情景发生的概率未知时,决策者需要知道的是各种策略在不同情景下的效益值,以及这些效益值与各种情景下最优策略的效益值的差别,这些信息是决策者合理决策的依据. 因此,鲁棒优化是基于对最坏情况优化的考虑,即所求解在最坏情况下依然保持优化特性. 鲁棒最优解不一定是某一情景下的最优策略,而是在所有情景下得到的效益值都可接受的策略[14]. 鲁棒优化可分为绝对鲁棒优化、相对鲁棒优化和偏差鲁棒优化[15],下面分别建立相应的鲁棒优化模型.

定义情景集 S,其元素 s 为一种可能发生的情景,即机场容量和各定位点容量的可能取值组合. S 一般为有限集,$|S|=q$,q 的值由各动态容量区间内的元素数确定. 设在情景 s 下,目标函数为:

$$P(s)=\sum_{F_a\in F_A}\sum_{t_i\in T}C_a(t_i)\delta_a(t_i)+\sum_{F_d\in F_D}\sum_{t_i\in T}C_d(t_i)\delta_d(t_i), \tag{10}$$

最优解为:

$$P^*(s)=\min\sum_{F_a\in F_A}\sum_{t_i\in T}C_a(t_i)\delta_a(t_i)+\sum_{F_d\in F_D}\sum_{t_i\in T}C_d(t_i)\delta_d(t_i). \tag{11}$$

绝对鲁棒优化的最优解满足在所有情景下的最大航班延误损失最小,优化函数为:

$$\min_{s\in S}\max P(s). \tag{12}$$

设 $r\in S$,偏差鲁棒优化的最优解满足在所有情景下与最小航班延误损失之差的最大值最小,优化函数为:

$$\min_{s\in S}\max_{r\in S}|P(s)-P^*(r)|. \tag{13}$$

相对鲁棒优化的最优解,在所有情景下与最小航班延误损失之差占最小航班延误损失比例的最大值最小时,优化函数为:

$$\min_{s\in S}\max_{r\in S}\left|\frac{P(s)-P^*(r)}{P^*(r)}\right|. \tag{14}$$

3　算法设计

鲁棒优化问题的求解需要综合考虑各种情景,计算量较大. 确定情景下的优化算法是整个求解过程的基础,直接影响求解效率,对算法性能要求较高. 捕食搜索算法(predatory search algorithm, PSA)[16]是一类新的仿生计算方法,该算法模拟动物的捕食策略,控制搜索空间的大小限制,实现局域搜索和全局搜索及其相互转换,具有很好的局部集中搜索和跳出局部最优的能力,已成功应用于旅行商[17]、超大规模集成电路设计[18]和车辆路径[19]等组合优化问题,但目前对该算法的应用研究仍不多[19]. 本文以捕食搜索算法为基础,寻找鲁棒最优解.

3.1　捕食搜索算法

捕食搜索算法的基本原理是:先在整个搜索空间进行全局搜索,直至找到一个较优解;然后在较优解附近区域集中搜索,直到搜索多次也找不到更

优解，从而放弃局域搜索；接着再在整个搜索空间进行全局搜索；如此循环，直到找到最优解（或近似最优解）为止. 搜索过程分两个步骤：

（1）全局搜索：搜索整个空间，如果找到猎物或有猎物存在的迹象，就转步骤（2）；

（2）局域搜索：在猎物的邻域内进行精密搜索，如果很长一段时间没有进展，则转步骤（1）.

采用基于时段排列的顺序编码，即对 n 个时间段分别产生进场和离场流量分配的整数序列，检验其可行性，从而形成一个可行解对应的顺序编码，例如：$\overbrace{2-3-\cdots-6}^{\text{进场航班}}-\overbrace{5-1-\cdots-2}^{\text{离场航班}}$（$t_1\ t_2\ \cdots\ t_n$）. 采用逆转法实现邻域操作，即随机选择解的两个位置，将它们之间的编码进行逆转，并剔除不可行解，得到当前解的一个邻域. 通过设置限制值实现算法的局域和全局搜索并进行转换是捕食搜索算法的重点. 本文采用 Linhares 提出的目标函数值限制法，即通过多次搜索当前较好解的邻域获得一组目标函数值，选取其中较小的部分值作为局域搜索限制，较大的部分值作为全局搜索限制.

设 *LEVEL_NUM* 为总限制值，*LOCAL_LEVEL* 为局域搜索限制，*GLOBAL_LEVEL* 为全局搜索限制，三者满足 *LEVEL_NUM* > *GLOBAL_LEVEL* > *LOCAL_LEVEL* > 0，*COUNTER_MAX* 为每个限制下的最大循环次数，W 为当前解邻域的搜索次数，参考文献[19]，捕食搜索算法的具体步骤如下：

步骤 1 随机产生一个初始解 x，令至今最优解 $x_{\min}=x$，限制级别 *Level* = 0，循环次数 *Counter* = 0.

步骤 2 如果 *Level* ≤ *LEVEL_NUM*，则搜索 x 的邻域 W 次，并取得临时最优解 $x_{n\_\min}$，然后，转步骤 3；否则，结束. $x_{\min}$ 即为求得的最优解.

步骤 3 如果 $f(x_{n\_\min})\leqslant$ Re *striction*(*Level*)，则令 $x=x_{n\_\min}$，然后，转步骤 4；否则，转步骤 5.

步骤 4 如果 $f(x)\leqslant f(x_{\min})$，则令 $x_{\min}=x$，*Level* = 0，*Counter* = 0，重新计算限制，然后，转步骤 2；否则，转步骤 5.

步骤 4 令 *Counter* = *Counter* + 1，如果 *Counter* > *COUNTER_MAX*，则令 *Level* = *Level* + 1，*Counter* = 0，然后，转步骤 6；否则，转步骤 2.

步骤 6 如果 *Level* = *LOCAL_LEVEL*，则令 *Level* = *GLOBAL_LEVEL*（通过限制级别 *Level* 的跳跃，实现从局域搜索到全局搜索的转换）；否则，直接转步骤 2.

每当解得到改善时，即获得一个至今最好的解，则执行以下操作计算限制：

（1）搜索 *LEVEL_NUM* 次存在至目前最好解的邻域，得到 *LEVEL_NUM* 个解的目标值；

（2）将这 *LEVEL_NUM* 个值与至今最好解的值按升序排列；

（3）将排列后的 *LEVEL_NUM* + 1 个值依次赋给限制 *Restriction*（0），*Restriction*（1），…，*Restriction*(*LEVEL_NUM*)；

（4）取其中 *Restriction*(0)，*Restriction*(1)，…，*Restriction*(*LOCAL_LEVEL*) 部分作为算法的局域搜索限制，而 *Restriction*（*GLOBAL_LEVEL*），…，*Restriction*(*LEVEL_NUM*) 部分作为算法的全局搜索限制.

3.2 求解鲁棒最优解

每个鲁棒优化函数均包含多个子优化函数，用捕食搜索算法求解每个子优化函数. 对于求最大值的子优化函数，将其转化为求最小值形式，3 种鲁棒最优解的求解步骤如图 2 所示.

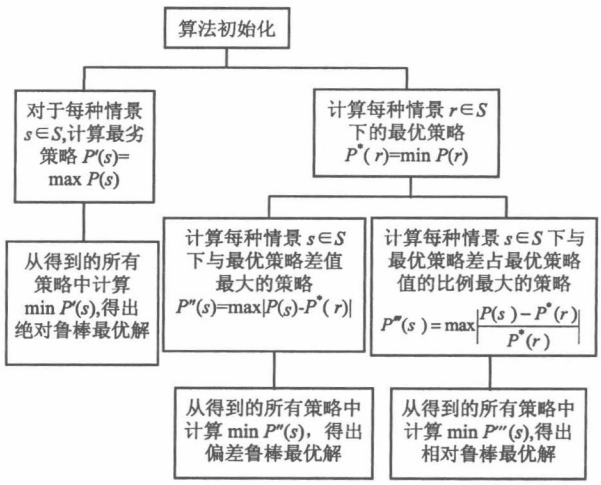

图 2 鲁棒最优解的求解流程

Fig. 2 Process of solving robust optimization

4 算例分析

设某机场进场和离场定位点数量均为 2，即 $J=K=2$. 未来时间区间（14:00 ~ 16:00，时段数 $n=8$，时段长度 $\Delta T=15$ min）内的空中交通需求见表 1. 受大雾等天气因素影响，该时间区间内各定位点和机场的容量发生相应变化，根据天气预报进行容量预测，动态容量预测区间见表 2. 表 1 和表 2 中需求、容量、流量的单位均为架. 可知定位点和机场的空中交通需求有时会完全或部分超出了动态

容量区间. 这种需求与容量的不匹配造成航班延误,动态容量的不确定性又增加了决策难度. 因此,需要合理分配流量,根据决策者规避风险的不同偏好,寻求在所有情景下的航班延误损失都可以接受的流量分配策略,供决策者选择.

应用捕食搜索算法求解子优化函数时,参数设置: $W=8$, $LEVEL\_NUM=16$, $LOCAL\_LEVEL=2$, $GLOBAL\_LEVEL=14$, $COUNTER\_MAX=120$. 航班延误损失按文献[10]所述方法确定. 计算得到该问题的绝对鲁棒最优解、偏差鲁棒最优解和相对鲁棒最优解,见表 3 ~ 5.

表 1　空中交通需求

Tab. 1　Air traffic demand　　架

时段	进场航班需求			离场航班需求		
	进场定位点 1	进场定位点 2	机场	离场定位点 1	离场定位点 2	机场
14:00 ~ 14:15	5	3	8	1	4	5
14:15 ~ 14:30	2	8	10	4	2	6
14:30 ~ 14:45	3	6	9	3	1	4
14:45 ~ 15:00	5	1	6	3	3	6
15:00 ~ 15:15	2	3	5	1	2	3
15:15 ~ 15:30	4	0	4	3	2	5
15:30 ~ 15:45	4	4	8	3	4	7
15:45 ~ 16:00	4	3	7	1	1	2
总计	29	28	57	19	19	38

表 2　动态容量预测区间

Tab. 2　Forecasting interval of dynamic capacity　　架

时段	进场定位点 1	进场定位点 2	离场定位点 1	离场定位点 2	机场
14:00 ~ 14:15	[6,9]	[6,9]	[6,9]	[6,9]	[13,16]
14:15 ~ 14:30	[6,9]	[6,9]	[6,9]	[6,9]	[13,16]
14:30 ~ 14:45	[3,6]	[3,6]	[4,7]	[4,7]	[12,16]
14:45 ~ 15:00	[2,4]	[3,6]	[4,7]	[3,6]	[10,13]
15:00 ~ 15:15	[2,4]	[2,4]	[2,4]	[2,4]	[7,10]
15:15 ~ 15:30	[2,4]	[2,4]	[2,4]	[2,4]	[7,10]
15:30 ~ 15:45	[5,8]	[5,8]	[5,8]	[5,8]	[9,12]
15:45 ~ 16:00	[6,9]	[6,9]	[6,9]	[6,9]	[13,16]

表 3　绝对鲁棒最优策略

Tab. 3　Strategy of absolute robust optimization

时段	进场航班流量分配				离场航班流量分配			
	进场定位点 1	进场定位点 2	机场	$P(s)$	离场定位点 1	离场定位点 2	机场	$P(s)$
14:00 ~ 14:15	5	3	8	0.0	1	4	5	0.0
14:15 ~ 14:30	2	6	8	68.7	4	1	5	28.7
14:30 ~ 14:45	3	3	6	204.3	3	2	5	0.0
14:45 ~ 15:00	2	3	5	243.1	2	3	5	27.2
15:00 ~ 15:15	2	2	4	317.8	2	1	3	42.5
15:15 ~ 15:30	2	2	4	341.6	1	2	3	67.3
15:30 ~ 15:45	5	4	9	309.5	0	0	0	158.6
15:45 ~ 16:00	6	5	11	84.6	1	1	2	139.4
总计	27	28	55	1 494.9	14	14	28	463.7

从结果可以看出，绝对鲁棒最优策略下的航班延误损失较其他两种鲁棒最优策略大得多，该策略比较保守. 决策者认为最坏情景出现时，易于选择绝对鲁棒最优策略，由于没有考虑各种情景下的最优解，绝对鲁棒最优解相对容易求解. 偏差鲁棒最优策略和相对鲁棒最优策略下的航班延误损失接近，这两种策略的鲁棒性相近，能将各情景下与最优策略的最大偏差控制到最小，从而在不确定环境下最大限度地规避风险，但求解相对复杂. 在情景集 C 中任选5种情景，即机场和定位点容量的5种组合，分别用遗传算法和捕食搜索算法求解各种情景下的流量优化分配策略. 设遗传算法的种群规模为100，进化代数为100，选择概率为0.3，交叉概率为0.8，变异概率为0.01，5种情景下求得最优解的平均计算时间为2.47 s；捕食搜索算法采用前文所述的参数设置，求得最优解的平均计算时间为1.92 s. 两种算法在各情景下的寻优结果一致，但捕食搜索算法耗时较短，因此，捕食搜索算法比遗传算法更高效. 限于篇幅，各情景下的流量最优分配策略及计算时间不再赘述.

表4 偏差鲁棒最优策略

Tab. 4 Strategy of deviation robust optimization

时段	进场航班流量分配				离场航班流量分配			
	进场定位点1	进场定位点2	机场	$P(s)$	离场定位点1	离场定位点2	机场	$P(s)$
14:00~14:15	5	3	8	0.0	1	4	5	0.0
14:15~14:30	2	7	9	35.2	4	1	5	28.7
14:30~14:45	3	5	8	132.7	3	2	5	0.0
14:45~15:00	3	3	6	118.5	2	3	5	27.2
15:00~15:15	3	3	6	64.9	2	1	3	42.5
15:15~15:30	3	0	3	126.2	2	3	5	22.1
15:30~15:45	5	4	9	62.1	1	0	1	151.3
15:45~16:00	5	3	8	0.0	3	3	6	76.9
总计	29	28	57	539.6	18	17	35	348.7

表5 相对鲁棒最优策略

Tab. 5 Strategy of relative robust optimization

时段	进场航班流量分配				离场航班流量分配			
	进场定位点1	进场定位点2	机场	$P(s)$	离场定位点1	离场定位点2	机场	$P(s)$
14:00~14:15	5	3	8	0.0	1	4	5	0.0
14:15~14:30	2	7	9	35.2	4	1	5	28.7
14:30~14:45	3	5	8	132.7	3	2	5	0.0
14:45~15:00	3	3	6	118.5	2	3	5	27.2
15:00~15:15	3	2	5	133.4	2	1	3	42.5
15:15~15:30	3	1	4	130.7	1	3	4	54.8
15:30~15:45	5	4	9	62.1	1	0	1	177.6
15:45~16:00	4	4	7	0.0	3	4	7	76.9
总计	28	29	57	612.6	17	18	35	407.7

5 结 论

天气等不确定因素增加了容量的不确定性，也增加了流量分配的难度，传统的基于静态容量的流量分配难以满足空中交通战术和预战术流量管理的要求. 本文以机场和定位点动态容量为研究背景，建立了鲁棒优化模型，寻求容量不确定条件下流量分配的满意策略，以一类新的仿生算法——捕食搜索算法为基础求解模型，分别得到绝对鲁棒最优策略、偏差鲁棒最优策略和相对鲁棒最优策略，根据对不确定程度的不同估计有效规避风险，为决策者提供了决策依据，也为空中交通战术和预战术流量管理提出了新思路.

虽然鲁棒优化方法可以很好地解决不确定优化问题，但涉及情景、策略数量大，问题较为复杂

时,鲁棒解的求解将变得很困难. 因影响因素的复杂性,动态容量的评估与预测也是一项难题. 充分掌握动态容量的不确定信息,研究不确定条件下容量流量分配问题将是下一步研究的重点.

参考文献:

[1] ANDRETT A G, ROMANIN G. Aircraft flow management under congestion[J]. Transportation Science, 1987, 21(3): 249-253.

[2] RICHETTA O, ODONI A R. Solving optimally the static ground holding policy problem in air traffic control [J]. Transportation Science, 1993, 27(3): 228-238.

[3] GILBO E P. Airport capacity: representation, estimation, optimization [J]. IEEE Transactions on Control Systems Technology, 1993, 1(3): 144-154.

[4] GILBO E P. Optimizing airport capacity utilization in air traffic flow management subject to constraints at arrival and departure fixes[J]. IEEE Transactions on Control Systems Technology, 1997, 5(5): 490-503.

[5] 余江,王大海,蒲云. 终端区起飞着陆的协同优化[J]. 系统工程学报,2003,18(5): 462-465.
YU Jiang, WANG Dahai, PU Yun. Coordinated optimization of terminal area landing and takeoff[J]. J. of Systems Engineering, 2003, 18(5): 462-465.

[6] 马正平,崔德光,谢玉兰. 机场终端区流量分配及优化调度[J]. 清华大学学报(自然科学版),2003, 43(7): 876-879.
MA Zhengping, CUI Deguang, XIE Yulan. Flow distribution and optimal scheduling in airport terminal area [J]. Journal of Tsinghua University (Sci. & Tech.), 2003, 43(7): 876-879.

[7] PAOLO D O, GUGLIELMO L. A dynamic programming approach for the airport capacity allocation problem[J]. IMA Journal of Management Mathematics, 2003, 14(3): 235-249.

[8] GILBO E P, HOWARD K W. Collaborative optimization of airport arrival and departure traffic flow management strategies for CDM[C]//3rd USA/Europe Air Traffic Management R&D Seminar. Napoli: [s. n.], 2000: 1-11.

[9] 张洪海,胡明华,陈世林. 机场进离场流量协同分配策略[J]. 南京航空航天大学学报,2008,40(5): 641-645.
ZHANG Honghai, HU Minghua, CHEN Shilin. Collaborative distribution strategy of airport arrival and departure traffic flow[J]. Journal of Nanjing University of Aeronautics & Astronautics, 2008, 40(5): 641-645.

[10] 张洪海,胡明华,陈世林. 机场终端区容量利用和流量分配协同优化策略[J]. 西南交通大学学报, 2009,44(1): 128-134.
ZHANG Honghai, HU Minghua, CHEN Shilin. Collaborative optimization of capacity utilization and flow assignment in airport terminal area[J]. Journal of Southwest Jiaotong University, 2009, 44(1): 128-134.

[11] 陈欣,陆迅,朱金福. 枢纽机场空侧容量利用和流量分配优化模型[J]. 南京航空航天大学学报,2007, 39(5): 680-684.
CHEN Xin, LU Xun, ZHU Jinfu. Optimization model of hub-airport airside capacity utilization and flow allocation [J]. Journal of Nanjing University of Aeronautics & Astronautics, 2007, 39(5): 680-684.

[12] ZOBELL S, WANKE C, SONG Lixia. Probabilistic airspace congestion management [C] // AIAA 5th Aviation, Technology, Integration, and Operations Conference. Arlington: [s. n.], 2005: 1-13.

[13] LEUNG S C, TSANG S O, NG W L, et al. A robust optimization model for multi-site production planning problem in an uncertain environment [J]. European Journal of Operational Research, 2007, 181(1): 224-238.

[14] BEN-TAL A, NEMIROVSKI A. Robust optimization-methodology and applications[J]. Mathematical Programming, 2002, 92(3): 452-480.

[15] YU G. Robust economic order quantity models[J]. European Journal of Operational Research, 1997, 100 (3): 482-493.

[16] LINHARES A. Preying on optimal: A predatory search strategy for combinatorial problems[C]//Proceeding of the IEEE International Conference on Systems, Man and Cybernetics, San Diego: [s. n.], 1998, 2974-2978.

[17] LINHARES A. State-space search strategies gleaned from animal behavior: A traveling salesman experiment [J]. Biological Cybernetics, 1998, 78: 167-173.

[18] LINHARES A. Synthesizing a predatory search strategy for VLSI layouts[J]. IEEE Transactions on Evolutionary Computation, 1999, 3(2): 147-152.

[19] 蒋忠中,汪定伟. 有时间窗车辆路径问题的捕食搜索算法[J]. 控制与决策,2007,22(1): 59-62.
JIANG Zhongzhong, WANG Dingwei. Predatory search algorithm for vehicle routing problem with time windows [J]. Control and Decision, 2007, 22(1): 59-62.

(中文编辑:秦萍玲　　英文编辑:兰俊思)

Safety Science 48 (2010) 926–930

Contents lists available at ScienceDirect

Safety Science

journal homepage: www.elsevier.com/locate/ssci

Estimation of air traffic longitudinal conflict probability based on the reaction time of controllers

Yang Shang-wen *, Hu Ming-hua

College of Civil Aviation, Nanjing University of Aeronautics and Astronautics, 29 Yudao Street, Nanjing, PR China

ARTICLE INFO

Article history:
Received 8 September 2009
Received in revised form 25 January 2010
Accepted 23 March 2010

Keywords:
Air traffic control
Conflict probability
Controller reaction time
Lognormal distribution

ABSTRACT

To estimate air traffic longitudinal conflict probability influenced by human factors, an analytic model considering the reaction time of controllers is proposed. In the model, the decelerating process of two close flights is described, and the reaction time of controllers is considered a stochastic variable. Then one hundred data of the controller reaction time are collected and analysed. Maximum likelihood estimate is used for parameter estimation. The Anderson–Darling Goodness of Fit test is used for significance test. The results show that the reaction time of controllers fits lognormal distribution at levels of significance 0.05, 0.025, 0.01 and 0.005 respectively. Case study is then performed to certify the rationality of the model, and the impact of the controller reaction time on air traffic longitudinal conflict probability is shown.

1. Introduction

For the application of satellite-based CNS (Communication Navigation Surveillance) and the improvement of aircraft performance, air traffic management is more highly human-dependent for its safety. Human behaviour plays a key role in air traffic management safety. Previous work on air traffic risk assessment, including original Reich model (Reich, 1966) and some typical examples such as stochastic model (Bakker and Blom, 1993) and EVENT model (Brooker, 2008), mainly focused on conflict or collision risks in longitudinal orientation, lateral orientation and vertical orientation caused by system errors, navigation errors and weather factors. There are also some achievements considering human factors in air traffic risk assessment. DNV (1997) estimated the safe spacing of P-RNAV parallel routes taking ATC intervention into account. Brooker (2008) studied spacing safety taking account of human factors and non-human factors through accident analysis, and demonstrated that collision risks caused by human factors accounted for the proportion of about 85%. However, literatures on quantified human behaviour in air traffic risk assessment are still rare.

As one of the main aspects in human behaviour, human error is a major contributor to air traffic management incidents, with some reviewers suggesting that human error contribution is in the order of 90% or more (Isaac et al., 2002). Since the probability of the occurrence of the errors is small, the probability distribution is difficult to formulate in a model. As Brooker (2008) say, it is inherently difficult to produce estimation of event frequency for infrequent occurrences. Although it is difficult to model the errors or the reliability of controllers, Human Reliability Assessment (HRA) in air traffic management has been carried out (Isaac et al., 2002). Kirwan et al. (2008) collected Human Error Probabilities (HEPs) via analysing the results of a real-time simulation involving controllers and pilots with a focus on communication errors, and discussed options and potential ways forward for the development of a full HRA capacity in air traffic management. Nevertheless, the real-time air traffic risk is difficult to assess according to the errors of controllers. The detailed tasks to be carried out by controllers during detection of air traffic conflict and separation loss has been split up into tasks performed by the perceptual, cognitive and motor processors (Mosquera-Benitez et al., 2009). Mosquera-Benitez et al. (2009) estimated the collision probability based on controller reaction time for potential conflicts in the scenario that a pair of aircraft encounter in cross routes. Wicks et al. (2005) applied Operator Choice Model (OCM) to the research on the controller reaction time for potential conflicts in cross routes, and demonstrated that the distribution of controller reaction time followed the geometric distribution.

In fact, the controller reaction time in the two literatures above shows the controller performance in conflict detection in cross routes. In this research, the controller reaction time concerned is a kind of stimulus–response time, which has been an important measure in the investigation of cognitive processes. We study the probability distribution of the reaction time of controllers monitoring the operations of air traffic, and propose a new model to

* Corresponding author. Tel.: +86 025 84896232.
E-mail address: swyang_08@yahoo.cn (S.-w. Yang).

0925-7535/$ - see front matter © 2010 Elsevier Ltd. All rights reserved.
doi:10.1016/j.ssci.2010.03.016

estimate longitudinal conflict probability. It is expected that the method would be useful as a reference for future theoretical research. The remainder of the paper is organized as follows. In Section 2, we formulate the model. In Section 3, we analyse the probability distribution of the reaction time of controllers. In Section 4, a case is studied, and we have a discussion. Finally, we conclude in Section 5.

2. Mathematical model

For the preferences of pilots and airlines or other reasons, aircraft may change their speed. Especially in route, there is less change in the altitude of a flight. When the leading aircraft decelerates, controllers need identify it and issue the instructions to the following aircraft in the same route and direction to decelerate. After certain delay which includes the time of identifying, thinking, determination, and communication, the following aircraft begins to decelerate. We define the time of identifying, thinking and determination as the reaction time of controllers.

The assumptions used for the model are listed below:

(1) The change of the speed for each aircraft is allowed by aircraft performance and ensures that the altitude of each aircraft will not be changed.
(2) Pilots execute the instructions of controllers immediately.
(3) The decelerating process terminates when the two aircraft reach the same final speed, and the final speed is known.
(4) Generally speaking, the time spent on decelerating in fixed altitude is short enough to make us believe that the deceleration of each aircraft is constant in the decelerating process.

Fig. 1 shows the decelerating process. At the time when the leading aircraft at the initial ground speed of v_l began to decelerate with the deceleration a_l, the separation between the leading aircraft and the following aircraft was s_0. Then the following aircraft began to decelerate with the deceleration a_f after the controller reaction time T and the communication time C, during which the following aircraft had advanced for a distance of s_1 at the initial ground speed of v_f. After having advanced for s_2, the two aircraft reaches the same ground speed v_t when the following aircraft has advanced for s_3. Now the decelerating process terminates, and the separation between them is s. The time spent by the leading aircraft on decelerating is t_l, and the time spent by the following aircraft on decelerating is t_f.

Then we can formulate relative equations as follows:

$$s_1 = v_f(T + C) \tag{1}$$

$$t_l = (v_l - v_t)/a_l \tag{2}$$

$$t_f = (v_f - v_t)/a_f \tag{3}$$

$$s_2 = \begin{cases} v_f t_f - \frac{1}{2} a_f t_f^2, & t_f + T + C \geqslant t_l \\ v_f t_f - \frac{1}{2} a_f t_f^2 + \\ v_t(t_l - t_f - T - C), & t_f + T + C < t_l \end{cases} \tag{4}$$

$$s_3 = \begin{cases} v_l t_l - \frac{1}{2} a_l t_l^2, & t_l - T - C > t_f \\ v_l t_l - \frac{1}{2} a_l t_l^2 + \\ v_t(t_f + T + C - t_l), & t_l - T - C \leqslant t_f \end{cases} \tag{5}$$

$$s = s_0 + s_3 - s_1 - s_2 \tag{6}$$

Define the longitudinal separation minima as *sep*. The longitudinal conflict probability p_c can be written as follows:

$$\begin{aligned} p_c &= P\{s < sep\} \\ &= P\left\{T > \left[s_0 + \left(v_l t_l - \frac{1}{2} a_l t_l^2\right) + v_t(t_f - t_l) - \left(v_f t_f - \frac{1}{2} a_f t_f^2\right) - sep\right]/(v_f - v_t) - C\right\} \\ &= 1 \\ &\quad - P\left\{T \leqslant \left[s_0 + \left(v_l t_l - \frac{1}{2} a_l t_l^2\right) + v_t(t_f - t_l) - \left(v_f t_f - \frac{1}{2} a_f t_f^2\right) - sep\right]/(v_f - v_t) - C\right\} \end{aligned} \tag{7}$$

3. The probability distribution of controller reaction time

If sufficiently good models of system processes and human observation, decision and response are available, then fast-time computer simulation is also an option, and is normally much cheaper than Human-In-The-Loop (HITL). However the literature supports relatively few areas amenable to quantitative dynamic models of human performance. Among these are visual and auditory signal detection, continuous control, statistical decision-making, and information processing. One particular issue that arises in Next Generation Air Transportation Systems (NGATS) is the fact that human decisions take time, and when humans are called upon to evaluate complex situations that are unexpected and off-normal the response time may be quite long. It is well known that the distribution of human response time fits a lognormal model quite well (Sheridan, 2006). For example, Taoka (1989) applied an analytical model using the lognormal probability density function to publish driver response time measurements, and close agreement was obtained when this function was fitted to the measured responses of drivers to the onset of the amber signal as they approached signalized intersections. Van Der Linder (2006) found that the lognormal model showed an excellent fit to the response time of a person on a set of test items.

It is known that lognormal distribution has been widely applied in many fields such as economics, biology, medicine, and materials. Suppose that there is a sample, of which every datum is larger than zero and could be very small positive value. When the number of the sample is large enough, that is, fifty or more, it could be assumed that the natural logarithm values of the sample fit or

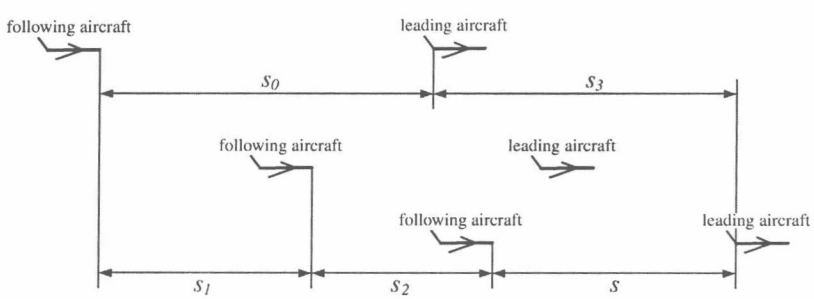

Fig. 1. The decelerating process of two close flights.

approximate normal distribution, which means that the sample fits or approximates lognormal distribution (D' Agostino and Stephens, 1986). The probability density function of lognormal distribution is then

$$F(x) = \begin{cases} \frac{1}{\sqrt{2\pi}x\xi} \exp\left[-\frac{(\ln x-\lambda)^2}{2\xi^2}\right], & x > 0 \\ 0, otherwise \end{cases} \quad (8)$$

where $\lambda = \ln\left(\frac{\mu}{\sqrt{1+\sigma^2/\mu^2}}\right)$, $\xi^2 = \ln\left(1+\frac{\sigma^2}{\mu^2}\right)$, and μ and σ are respectively defined as the mean and the variance of the sample.

We experiment on the air traffic control simulator designed according to real operations of an air traffic control centre, and collect one hundred data in different air traffic conditions including peak hours and common periods. The raw data are listed in Table 1.

We use the common mathematical software Matlab6.5 to analyse and process the data of T. The histograms of T and $\ln T$ are shown in Figs. 2 and 3 respectively.

We can see that $\ln T$ seems to fit or approximately fit normal distribution. We assume that both T and $\ln T$ fit the normal distribution. Then the maximum likelihood estimates for these parameters can be written as follows:

$$\hat{\mu} = \frac{\sum_{i=1}^{n} T_i}{n} = 2.31 \quad (9)$$

$$\hat{\sigma} = \sqrt{\frac{\sum_{i=1}^{n}(T_i - \hat{\mu})^2}{n}} = 0.223 \quad (10)$$

$$\hat{\lambda} = \frac{\sum_{i=1}^{n} \ln T_i}{n} = 0.83 \quad (11)$$

$$\hat{\xi} = \sqrt{\frac{\sum_{i=1}^{n}(\ln T_i - \hat{\lambda})^2}{n}} = 0.0943 \quad (12)$$

where n is the size of the sample.

Then we carry out significance test. Normal distribution and lognormal distribution are best tested by use of the Anderson–Darling Goodness of Fit test. The A–D test is designed to detect differences in the tails between the fitted distribution and the data. The A–D test statistic is a weighted average of the squared difference between the Empirical Distribution and the fitted cumulative distribution function. The A–D test is usually considered to be more powerful than either the chi-square or Kolmogorov Smirnov tests. The A–D test statistic is defined as

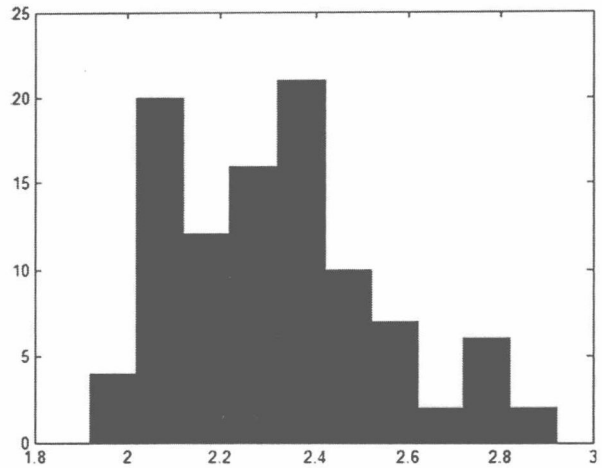

Fig. 2. The histogram of T.

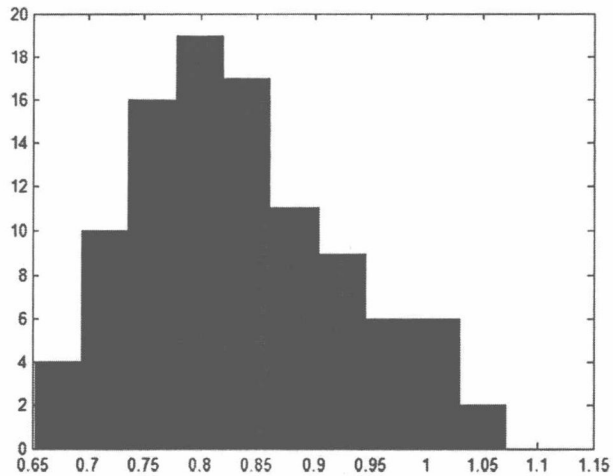

Fig. 3. The histogram of $\ln T$.

Table 1
The reaction time of controllers.

No.	Reaction time (s)	No.	Reaction time (s)	No.	Reaction time (s)	No.	Reaction time (s)	No.	Reaction time (s)
1	2.34	21	2.13	41	2.34	61	2.35	81	2.10
2	2.62	22	2.19	42	2.16	62	2.15	82	1.97
3	2.29	23	2.09	43	2.27	63	2.04	83	2.09
4	2.38	24	2.33	44	2.47	64	2.12	84	2.42
5	2.40	25	2.04	45	2.34	65	2.79	85	2.79
6	2.25	26	2.23	46	2.04	66	2.25	86	2.58
7	2.35	27	2.10	47	2.24	67	2.76	87	2.25
8	2.49	28	2.09	48	2.04	68	2.25	88	2.35
9	2.92	29	2.75	49	2.34	69	2.05	89	2.26
10	2.08	30	2.58	50	2.28	70	2.13	90	2.44
11	2.89	31	2.23	51	1.98	71	2.38	91	2.06
12	2.41	32	2.43	52	2.78	72	2.06	92	2.51
13	2.53	33	2.24	53	2.38	73	2.77	93	2.25
14	2.49	34	2.06	54	2.34	74	2.11	94	2.53
15	2.49	35	1.98	55	2.10	75	2.03	95	2.41
16	2.35	36	2.18	56	2.11	76	2.18	96	2.63
17	2.64	37	1.92	57	2.35	77	2.13	97	2.24
18	2.18	38	2.29	58	2.20	78	2.44	98	2.50
19	2.25	39	2.61	59	2.44	79	2.34	99	2.35
20	2.12	40	2.33	60	2.53	80	2.17	100	2.18

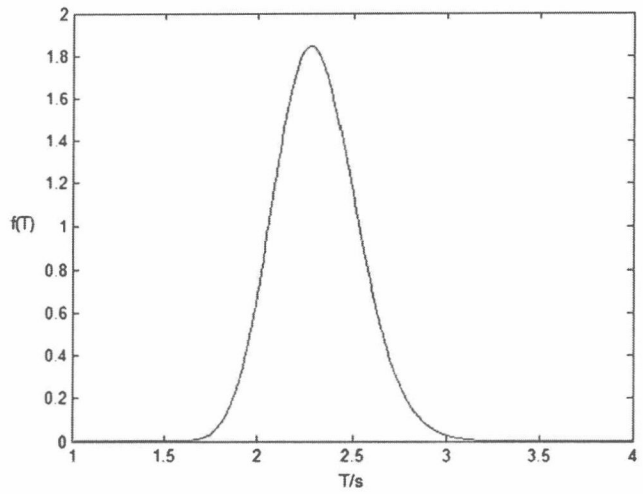

Fig. 4. The probability density function curve of T.

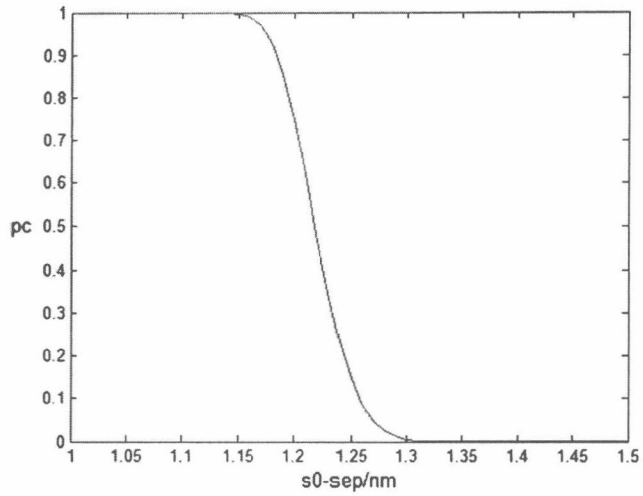

Fig. 5. The relation between s_0-sep and p_c.

$$A^2 = -n - \frac{1}{n}\sum_{i=1}^{n}(2i-1)(\ln F(Y_i) + \ln(1 - F(Y_{n+1-i}))) \tag{13}$$

where F is the cumulative distribution function of the assumed distribution, and Y_i are the ordered data (D' Agostino and Stephens, 1986).

Then the A^2 of T is 1.162, and the A^2 of $\ln T$ is 0.738. For samples of size $n \geqslant 8$, reject the null hypothesis of normality if A^2 exceeds 0.752, 0.873, 1.035, and 1.159 at levels of significance 0.05, 0.025, 0.01, and 0.005 respectively (D' Agostino and Stephens, 1986). Therefore, it is shown that $\ln T$ fits normal distribution at levels of significance 0.05, 0.025, 0.01, and 0.005 respectively, that is, T fits lognormal distribution.

The probability density function of T can be written as follows:

$$F(T) = \begin{cases} \frac{1}{0.236T}\exp\left[-\frac{(\ln T - 0.83)^2}{0.0178}\right], & T > 0 \\ 0, otherwise \end{cases} \tag{14}$$

The curve of the probability density function is shown in Fig. 4. Furthermore, the interval estimates for λ and ξ are [0.816, 0.853] and [0.0828, 0.1095] respectively at the level of significance 0.05. The interval estimates at other significance levels are not listed in detail.

4. Case study

To test how well the model may be applied in the real world, we perform numerical tests based on the experiment condition mentioned above. We choose two close flights in FL 290. The leading aircraft is B757-200 at a ground speed v_l of 455 knots, and the following aircraft is B737-300 at a ground speed v_f of 471 knots. The initial separation s_0 between them is 4.4 nm. The final ground speed v_t is 300 knots. According to aircraft performance manuals and pilot experience, the decelerations of the two aircraft a_l and a_f are 8 m/s^2 and 10 m/s^2 respectively. Although there may be some errors in the values of the decelerations, the errors would not affect the calculation of the conflict probability. As they are both medium types, the longitudinal separation minima sep is 3 nm according to International Civil Aviation Organization (ICAO) wake vortex separation minima. The voice communication time C is estimated to be an average of 7 s (Cullen, 1999). Then we calculate the longitudinal conflict probability p_c according to Eqs. (7) and (14):

$$p_c = 1 - \int_{-\infty}^{3.69} \frac{1}{0.236\sqrt{2\pi}T}\exp\left[-\frac{(\ln T - 0.83)^2}{0.0178}\right]dT = 2.89 \times 10^{-7}$$

Due to the change of the speed and the decelerating time in fixed altitude being confined, the differentials between s_2 and s_3 are small. We can find in the calculating process that the initial separation s_0 between the two aircraft and the ground speed differentials between v_f and v_t play an important role in the estimation of longitudinal conflict probability. We can see from Fig. 5 that p_c approximates 0 infinitely with the increase of s_0-sep.

The collision probability estimated in this method is smaller than 10^{-14}, that is to say, it may not be appropriate to assess collision risk in this method. Conflict probability and collision probability both reflect the safety of air traffic separation. Conflict probability mainly focuses on real-time air traffic safety, and collision probability mainly focuses on total air traffic safety. Conflict probability is generally formulated in the functions of time, and the research on conflict probability is devoted to predicting real-time conflict probability, analysing the workload of controllers, and so on. The research on collision risk is devoted to the safety of air traffic system and the possibility of reducing the separation minima, and the data used in analyses originate from the accumulation for years. The method proposed in this paper could be applied to predicting real-time longitudinal conflict probability. As mentioned above, s_0-sep and v_f–v_t play an important role in the method. Although there is no criterion on air traffic conflict risk, the method could be used to determine the safe separation according to the condition of an air traffic control center itself, including the air traffic situation and the condition of controllers.

5. Conclusions

In view of the difficulty in modelling the errors or reliability of controllers, we introduce the reaction time of controllers into estimating longitudinal conflict probability and propose an analytic model. After collecting and analysing the experiment data, we find that the reaction time of controllers fits lognormal distribution well. Then we apply the model to predicting the longitudinal conflict probability in real operations. The model provides a new way to study air traffic risks influenced by human factors. Although